Meteorol. Atmos. Phys. 61, 89–106 (1996)

Meteorology and Atmospheric Physics

[1] Fraunhofer-Institut für Atmosphärische Umweltforschung (IFU), Garmisch-Partenkirchen, Federal Republic of Germany
[2] Meteorologisches Institut der Ludwig-Maximilians-Universität, München, Federal Republic of Germany
[3] Deutscher Wetterdienst, Meteorologisches Observatorium Lindenberg, Dezernat Landoberflächenprozesse und Grenzschicht, Lindenberg, Federal Republic of Germany
[4] GSF-Research Center, Institute for Plant-Pathology, Oberschleißheim, Federal Republic of Germany

A SVAT Scheme for NO, NO_2, and O_3 – Model Description and Test Results

G. Kramm[1], N. Beier[2], T. Foken[3], H. Müller[1], P. Schröder[4], and W. Seiler[1]

With 9 Figures

Received February 20, 1995
Revised January 22, 1996

Summary

A soil/vegetation/atmosphere transfer (SVAT) scheme for determining the dry deposition and/or emission fluxes of NO, NO_2, and O_3 in the atmospheric surface layer over horizontally uniform terrain covered with fibrous canopy elements is presented and discussed. This transfer scheme is based on the micrometeorological ideas of the transfer of momentum, heat and matter near the Earth's surface, where chemical reactions between these trace gases are included. The fluxes are parameterized by first-order closure principles. The uptake processes by vegetation and soil are described in accord with Deardorff (1978). The SVAT scheme requires only routine data of wind speed, dry- and wet-bulb temperatures, short wave and long wave radiation, and the concentrations of O_3 and nitrogen species provided by stations of monitoring networks.

First model results indicate that the dry deposition fluxes of NO, NO_2, and O_3 are not only influenced by meteorological and plant-physiological parameters, but also by chemical reactions between these trace species and by NO emission from the soil. Furthermore, a small displacement in the concentrations of NO, NO_2, and O_3 within in the range of the detection limits of the chemical sensors can produce large discrepancies in the flux estimates, which are manifested here by the shift from height-invariant fluxes substantiated by the photostationary state to strongly height-dependent fluxes caused by the departure from that state. Especially in the case of these nitrogen species the widely used 'big leaf' multiple resistance approach, which is based on the constant flux approximation seems to be inappropriate for computing dry deposition fluxes and deposition velocities.

1. Introduction

It is well established that dry deposition plays an important role in the mass budget of many gaseous species (Businger, 1986). This removal process generally depends on the micrometeorological transfer properties of the atmospheric surface layer, the capability of vegetation and soil to take up matter, and the prevailing chemical and photochemical environment. It can directly be determined by eddy correlation techniques and/or by enclosure techniques (static and dynamic chamber systems). Eddy flux measurements require high-resolution physico-chemical analysis procedures, which have been developed for only a few trace gases, such as water vapour, SO_2, CO_2, NO, NO_2, and O_3 (e.g., Lenschow and Hicks, 1989). The technical requirements and the computer data management for these measuring techniques are considerable, but their results are representative for areas of several hectares extending upwind of the instruments (e.g., Delany et al.,

1986). Moreover, a prescription is required to interrelate the eddy fluxes well above the ground to those at the surfaces of vegetation and the soil, where the processes of deposition and emission take place.

On the contrary, measurements by enclosure techniques provide results of deposition or emission fluxes being representative only for small areas of up to a square metre (e.g., Slemr and Seiler, 1984). Representative results for larger areas can only be achieved with an array of chambers. Then, however, the technical requirements rapidly increase and may also exceed those for measuring eddy fluxes. Enclosure techniques are also inherently limited because they alter the local environment around the subject under study, in complete contrast to micrometeorological techniques (Baldocchi et al., 1988).

Since dry deposition tends to be extremely difficult to measure, the corresponding data set is still meager. Most flux estimates originate from individually conducted field experiments rather than from monitoring networks. To determine dry deposition by means of monitoring networks, mathematical models have to be used, which calculate the fluxes of atmospheric trace constituents on the basis of measured mean concentrations as well as mean meteorological quantities.

Currently, the inferential method seems to be the best available modelling tool to estimate dry deposition from monitoring data measured at a reference height z_R above ground. It is based on the flux-resistance analogy of the so-called constant flux theory for chemically conservative atmospheric trace gases expressed by (e.g., Wesely and Hicks, 1977)

$$F_i = -v_{d,i} c_{R,i} = \text{const.} \tag{1}$$

Here, F_i is the height-invariant vertical flux (density), $v_{d,i} = (r_{t,i} + r_{mt,i} + r_{s,i})^{-1}$ is the deposition velocity, and $c_{R,i} = c_i(z_R)$ is the mean concentration at the height z_R. Furthermore, $r_{t,i}$ is the bulk resistance of the turbulent region of the atmospheric surface layer against mass transfer, $r_{mt,i}$ is the corresponding bulk resistance of the underlying molecular-turbulent sublayer, and $r_{s,i}$ is the bulk resistance of the canopy which characterizes the biochemical and physical processes taking place in the soil and within the plants.

Equation (1) was used, for instance, by Hicks et al. (1987) to infer dry deposition fluxes of SO_2, HNO_3, O_3, and particles on the basis of routine data on species concentrations, wind speed, standard deviation of the wind direction, temperature, humidity and global radiation.

Results from recent field experiments over agricultural crop fields and unmanaged grassland at different sites (e.g., Delany et al., 1986; Hicks and Matt, 1988) indicate that in the case of the highly reactive trace gases NO and NO_2 (which are related to O_3 by chemical reactions) the eddy fluxes directly measured and the mean concentrations concurrently determined disagree with the flux-resistance relationship expressed by Eq. (1). As pointed out by Delany et al. (1986) and Hicks and Matt (1988), some disagreement could be caused by emission of NO and NO_2 from the soil. Results from model studies (e.g., Fitzjarrald and Lenschow, 1983; Kramm et al., 1991; Gao et al., 1991) also suggest that especially the fluxes of NO and NO_2 can strongly vary with height because flux divergences can occur which are caused by chemical reactions between NO, NO_2, and O_3. Thus, some disagreement could also be attributed to these chemical reactions.

In view of these facts it is obvious that the use of the Eq. (1) to describe the exchange of NO and NO_2 between the atmosphere and the biosphere could give false results, because $r_{t,i}$, at least, is not definable for chemically reactive trace species. Moreover, the applicability of Eq. (1), especially in chemical transport models like RADM (Chang et al., 1987), where the turbulent resistance, $r_{t,i}$, is calculated for the lowest layer of the atmosphere of a thickness of several decameters, seems to be inadequate.

In our study, a SVAT scheme for estimating the exchange of NO, NO_2, and O_3 is presented, where in contrast to Eq. (1), chemical reactions between these gases and NO emission are considered. This method is based on (a) an improved Deardorff-type SVAT scheme, which provides, among other things, the stomatal resistances for water vapour and trace gases using Jarvis's (1976) approach as well as the atmospheric fluxes of momentum, sensible and latent heat and the soil fluxes of sensible heat and moisture (Deardorff, 1978), and (b) the flux-resistance analogy for the canopy layer and the molecular-turbulent sublayer. The SVAT scheme has been tested on the basis of field data obtained over low vegetation (sugar beet) at Jülich/Germany in September 1984 (Höfken

et al., 1986). Sensitivity studies with different NO soil concentrations have been performed to demonstrate the effects of NO emission.

2. Model Description

2.1 The Flux-Resistance Relationship

2.1.1 The Atmospheric Resistances

Analogous to the empirical mixing laws of micrometeorology, the flux F_i of a trace gas entity is written as (Sheppard, 1958)

$$F_i = -(D_i + K_i)\frac{\partial c_i}{\partial z}, \tag{2}$$

where D_i is the molecular diffusivity, K_i is the respective eddy diffusivity, and $\partial c_i/\partial z$ is the vertical gradient of the (volumetric) concentration. Based on some empirical results that the turbulent transfers of sensible heat and water vapour are similar (e.g., Högström, 1967; Dyer and Hicks, 1970), which is adopted to the other scalars as well (e.g., Businger, 1986), it is assumed that K_i is equal to K_h, the eddy diffusivity of heat. This also agrees with empirical results derived from concurrent measurements of O_3 fluxes and O_3 profiles (Droppo, 1985).

Integrating Eq. (2) over the constant flux layer, $z_s \leqslant z \leqslant z_R$, provides (e.g., Herbert, 1987)

$$F_i = -r_{a,i}^{-1}(c_{R,i} - c_{s,i}) = \text{const.}, \tag{3}$$

where $c_{s,i}$ is the concentration at the height of the receptor surface, z_s, and $r_{a,i} = r_{t,i} + r_{mt,i}$ is the bulk resistance of the air against mass transfer. The resistances $r_{t,i} = r_t$ and $r_{mt,i}$ can be written as (e.g., Hicks, 1976)

$$r_t = \int_{\delta}^{z_R} K_h^{-1}\, dz = \frac{1}{u_* \kappa}\left(\ln\frac{z_R - d}{\delta - d} - \Psi_h(\zeta_R, \zeta_\delta)\right), \tag{4}$$

and (e.g., Owen and Thomson, 1963; Herbert, 1987)

$$r_{mt,i} = \int_{z_s}^{\delta} (D_i + K_h)^{-1}\, dz = (u_* B_i)^{-1}, \tag{5}$$

with (Schlichting, 1965; Kramm and Dlugi, 1994)

$$B_i^{-1} = Sc_i \underbrace{\int_0^{\eta_\delta} \frac{d\eta}{1 + Sc_i K_m/\nu}}_{I(Sc_i, \eta_\delta)} = Sc_i I(Sc_i, \eta_\delta)$$

$$= \frac{c_{\delta,i} - c_{s,i}}{c_{*,i}}. \tag{6}$$

Here, u_* is the friction velocity, $\kappa = 0.4$ is the von Kármán constant, $\delta > d$ is the outer edge of the molecular-turbulent sublayer, d is the zero-plane displacement, $\Psi_h(\zeta_R, \zeta_\delta)$ is the non-dimensional integral stability function for heat (Paulson, 1970; Kramm and Herbert, 1984), $\zeta = (z - d)/L$ (L is the Monin-Obukhov stability length) is a non-dimensional height, K_m is the eddy diffusivity for momentum, ν is the kinematic viscosity, $Sc_i = \nu/D_i$ is the Schmidt number, $\eta = u_*(z - z_s)/\nu$ is the roughness Reynolds number (or a non-dimensional height), $\eta_\delta = u_*(\delta - z_s)/\nu$ is the non-dimensional thickness of the molecular-turbulent sublayer, $c_{\delta,i}$ is the concentration at the height δ, and $c_{*,i}$ is the flux concentration related to the flux by $F_i = -u_* c_{*,i}$. The quantity B_i is the sublayer-Stanton number for the molecular-turbulent sublayer bordering the receptor surface. The quantities r_t and L are related to the turbulent height-invariant scaling parameters u_*, Θ_* (heat flux temperature) and q_* (water vapour flux concentration) which can similarly be determined on the basis of wind speed (U), potential temperature (Θ), and specific humidity (q) at the heights δ and z_R.

As indicated by Eq. (6), the sublayer-Stanton number is a measure of the difference in the transfer rates of momentum and matter to and from rough (e.g., Owen and Thomson, 1963; Schlichting, 1965) and smooth surfaces (e.g., Brutsaert, 1975; Kramm et al., 1992), respectively. The causes of this difference are (a) momentum is destroyed at the surface by skin friction and form drag, and only the former has an analogy in mass and heat transfer, and (b) the molecular diffusion coefficient is not numerically equal to the analogous kinematic viscosity (Chamberlain, 1968). The quantity B_i can be considered to be a function of the roughness Reynolds number and the Schmidt number of the material being transferred.

There are several parameterization approaches for B_i derived from laboratory and field studies, which strongly differ from each other (e.g., Garratt and Hicks, 1973; Beljaars and Holtslag, 1991). These B_i-relationships are controversially discussed (Kramm et al., 1995) and require further consideration. However, to calculate the molecular-turbulent resistances $r_{mt,fg,i}$ and $r_{mt,i}$ (see Fig. 1), in this study (a) the modified Owen and Thomson relationship (Owen and Thomson, 1963)

$$B_i^{-1} = a Sc_i^b \eta_\delta^c, \tag{7}$$

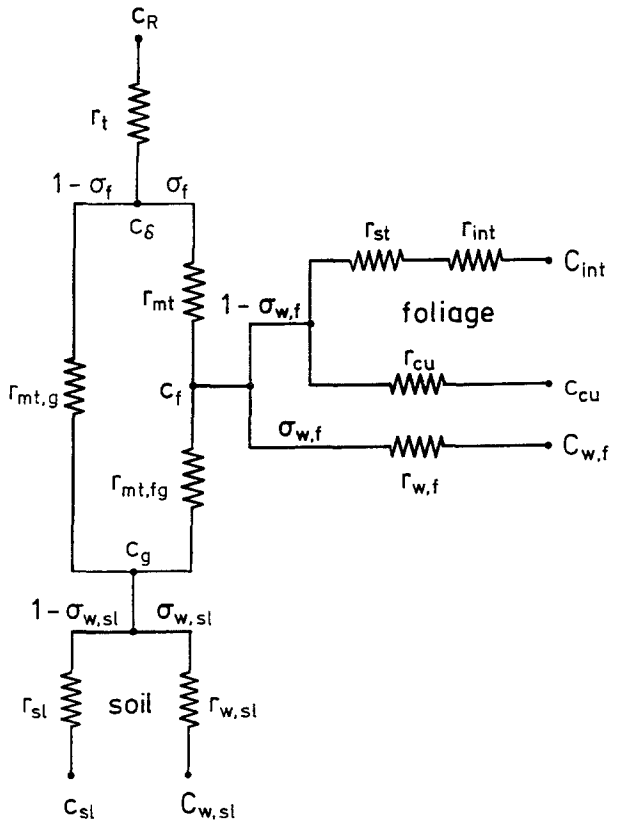

Fig. 1. Resistance network for describing the exchange of trace species between the atmosphere and the vegetation-soil system (Kramm and Dlugi, 1994)

with $a=0.52$, $b=0.8$, $c=0.45$, and $\eta_\delta = u_*(z_0+d)/\nu$ for the molecular-turbulent sublayer over an aerodynamically rough surface (Kramm and Herbert, 1984), and (b) Reichardt's (1951) approach for that over an aerodynamically smooth surface,

$$\frac{K_m}{\nu} = \kappa\left(\eta - \eta_D \tanh\frac{\eta}{\eta_D}\right), \tag{8}$$

are considered. Here, $\eta_D = 11$ is an empirical constant. Obviously, Reichardt's approach is able to describe the transition range from a purely viscous to the fully turbulent transfer. It is similar to the so-called film model (i.e., a layer of molecular transport at the interface, bordering on the bulk fluid with a region of fully turbulent transport), but avoids the unrealistic notion of a purely molecular layer near a fully turbulent layer and the necessity to determine its thickness (see also Hasse, 1971; Deacon, 1977).

2.1.2 Atmosphere – Biosphere Interaction

The flux F_i at the interface atmosphere-biosphere can be parameterized for low, horizontally homogenous vegetation as follows (see Fig. 1):

Foliage surface:

$$F_{f,i} = -\frac{c_{f,i} - H_i C_{int,i}}{r_{st,i} + H_i r_{int,i}} - \frac{1}{r_{cu,i}}(c_{f,i} - c_{cu,i}) - \frac{1}{H_i r_{w,f,i}}(c_{f,i} - H_i C_{w,f,i}) \tag{9}$$

with $r_{st,i} = r^*_{st,i}/(1-\sigma_{w,f})$, $r_{\mathrm{int},i} = r^*_{\mathrm{int},i}/(1-\sigma_{w,f})$, $r_{cu,i} = r^*_{cu,i}/(1-\sigma_{w,f})$, and $r_{w,f,i} = r^*_{w,f,i}/\sigma_{w,f}$.

Ground surface:

$$F_{g,i} = -\frac{1}{r_{sl,i}}(c_{g,i} - c_{sl,i}) - \frac{1}{H_i r_{w,sl,i}}(c_{g,i} - H_i C_{w,sl,i}) \tag{10}$$

with $r_{sl,i} = r^*_{sl,i}/(1-\sigma_{w,sl})$ and $r_{w,sl,i} = r^*_{w,sl,i}/\sigma_{w,sl}$. Here, $c_{f,i}$ and $c_{g,i}$ are the surface concentrations of the foliage and the ground, $r^*_{st,i}$ is the stomatal resistance, $r^*_{\mathrm{int},i}$ is the internal resistance, $r^*_{cu,i}$ is the cuticular resistance, $r^*_{sl,i}$ is the resistance of nearly dry soil, $r^*_{w,f,i}$ and $r^*_{w,sl,i}$ are the resistances of water (leaf wetness and soil water etc.), and $\sigma_{w,f}$ and $\sigma_{w,sl}$ ($0 \leqslant \sigma_w \leqslant 1$ for both cases) represent fractional foliage surface and fractional ground surface covered by water, respectively. The quantities $C_{int,i}$, $c_{cu,i}$, $c_{sl,i}$, $C_{w,f,i}$ and $C_{w,sl,i}$ are the substrate concentrations, where $C_{\mathrm{int},i}$, $C_{w,f,i}$ and $C_{w,sl,i}$ refer to aqueous solutions, and H_i is the non-dimensional Henry's law constant.

In our study the bulk stomatal resistance is estimated by use of Jarvis' (1976) parameterization scheme on the functional relationship between $r^*_{st,i}$ and the photosynthetically active radiation (PAR, in W m^{-2}) rearranged to (e.g., Sellers, 1987; Hicks et al., 1987)

$$r^*_{st,i} = \frac{r_{st,\min}\left(1 + \dfrac{b_{st}}{\mathrm{PAR}}\right)}{g_\delta(\delta_e) g_\psi(\psi) g_T(T_f) g_C(\mathrm{CO_2}) g_{D,i}}, \tag{11}$$

where $r_{st,\min}$ is the minimum value of $r^*_{st,i}$ at optimal conditions, and b_{st} is an empirical constant. Both quantities depend on the plant species. The functions $g_\delta(\delta_e)$, $g_\psi(\psi)$, $g_T(T_f)$, and $g_C(\mathrm{CO_2})$ ranging from 0 to 1 were introduced by Jarvis (1976) to correct $r^*_{st,i}$ with respect to effects of humidity,

water stress, temperature and carbon dioxide, respectively (see Appendix A).

The transfer through stomata is performed by molecular diffusion. Thus, in Eq. (11) the case of trace gases can be addressed by a simple correction factor $g_{D,i} = D_i/D_0$, where D_o refers to the molecular diffusivity at the initial values for $r_{st,\min}$ and b_{st} (usually that for water vapour), and D_i is the molecular diffusivity of the respective gas (e.g., Hicks et al., 1987).

In contrast to the stomatal resistance which can be estimated with sufficient accuracy, there exist only rough estimates for the resistances $r^*_{\text{int},i}$, $r^*_{cu,i}$, $r^*_{sl,i}$, $r^*_{w,f,i}$, and $r^*_{w,sl,i}$ (Wesely, 1989); but these quantities are assumed to be usually larger than the stomatal resistance, except for highly water-soluble trace gases like HNO_3 where the 'effective' resistances $H_i \cdot r^*_{\text{int},i}$, $H_i \cdot r^*_{w,f,i}$, and $H_i \cdot r^*_{w,sl,i}$ are much smaller.

In the case of low vegetation leaf resistances may be scaled according to the unit area of the ground surface (as a first approximation) by the amphistomatous leaf area index (LAI) (e.g., Hicks et al., 1987; Hanson and Lindberg, 1991). For taller vegetation and tree canopies with highly varying leaf area density (which leads to varying sorption conditions), it appears to be necessary to divide the canopy layer into several foliage layers, where for each foliage layer a resistance network analogous to that shown in Fig. 1 can be used, and where the exchange between the adjoining foliage layers can be described on the basis of a molecular-turbulent resistance similar to $r_{mt,fg,i}$ denoting the exchange between the lowest foliage layer and the ground.

As pointed out by Deardorff (1978), there is a rough relation between the shielding factor σ_f ($0 \leqslant \sigma_f \leqslant 1$) associated with the degree to which the foliage prevents shortwave radiation from reaching the ground and the one-sided leaf area index given by $\text{LAI} = 7\ \sigma_f$, which is consistent with results derived by Allan and Lemon (1972) for a corn crop and by Monteith et al. (1965) for barley. Assuming $\sigma_f = 1$ and taking Eqs. (3), (9), and (10) as well as $c_{s,i} = c_{f,i}$ into account, the flux, $F_i\,(= F_{f,i})$ can be specified by (Kramm et al., 1991)

$$F_i = -v^*_{d,i} c_{R,i} = \text{const.} \tag{12}$$

with $v^*_{d,i} = v_{d,i}\,(1 - \mu_i)$, where $v^*_{d,i}$ is denoted as an exchange velocity at the height z_R which is referred to the highest amount of the deposition velocity, $v_{d,i}$ (given by Eq. (1)), by the expression $1 - \mu_i$. As shown in Kramm et al. (1991) as well as Kramm and Dlugi (1994), the quantities $r_{s,i}$ and μ_i in Eq. (12) can be derived from Eqs. (9) and (10).

2.2 Temperature and Moisture at the Surfaces of Foliage and Soil

The following flux budget equations for energy and moisture are used to calculate the temperature and the specific humidity at the surfaces of foliage and soil as required by the model:

2.2.1 Energy Budget of Foliage Surface

$$\begin{aligned} F_1((T_f, T_g, \eta_g)^T) = {} & R_{S,f}\downarrow - R_{S,f}\uparrow + R_{L,f}\downarrow \\ & - R_{L,f}\uparrow - (R_{S,g}\downarrow - R_{S,g}\uparrow) \\ & - (R_{L,g}\downarrow - R_{L,g}\uparrow) \\ & - (H_f + L_v(T_f) Q_f) = 0 \end{aligned} \tag{13}$$

2.2.2 Energy Budget of Soil Surface

$$\begin{aligned} F_2((T_f, T_g, \eta_g)^T) = {} & R_{S,g}\downarrow - R_{S,g}\uparrow + R_{L,g}\downarrow - R_{L,g}\uparrow \\ & - (H_g + L_v(T_g) Q_g) + H_s = 0 \end{aligned} \tag{14}$$

2.2.3 Water Budget of Soil Surface

$$F_3((T_f, T_g, \eta_g)^T) = W_s - Q_g = 0 \tag{15}$$

Here, R_S and R_L are the fluxes of shortwave and longwave radiation, where the values at the top of the canopy are denoted by subscript f, those at the ground by subscript g. The arrows $\downarrow$ and $\uparrow$ denote the direction of these fluxes. The quantities H and $L_v(T)\ Q$ are the fluxes of sensible and latent heat within the atmosphere, where Q is the water vapour flux and $L_v(T)$ is the temperature-dependent latent heat of vaporization, H_s and W_s are the total fluxes of heat and moisture within the soil, T_f and T_g are the surface temperatures of foliage and soil, and η_g is the volumetric moisture content at the soil surface, which is required to determine the corresponding specific humidity, q_g. In accord with Monteith (1975), Deardorff (1978), and Müller et al. (1993), the heat storage of the canopy has been neglected in our study. Furthermore, the specific humidity within the stomatal cavities was assumed to be saturated ($q_i = q_i(T_f)$), even though experimental data indicate possible deviations from this "ideal" state (Ward and Bunce, 1986).

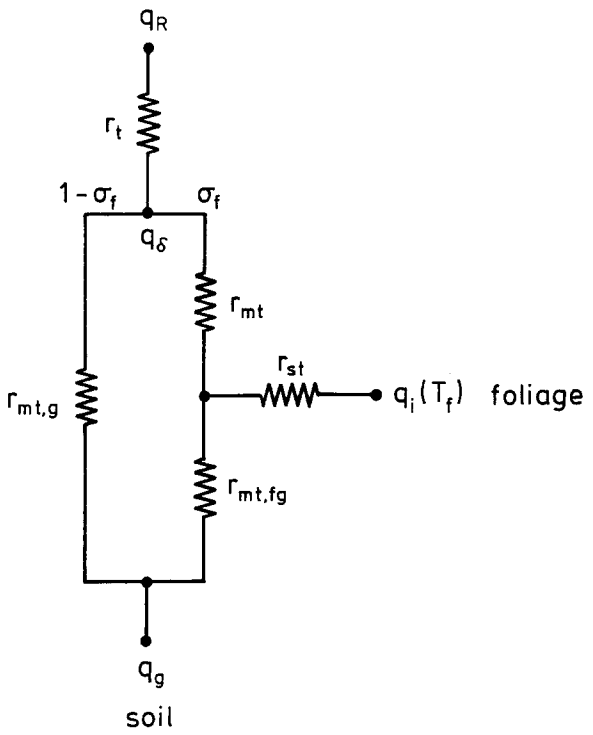

Fig. 2. Resistance network for describing the exchange of water vapour and sensible heat between the atmosphere and the vegetation-soil system. Note that in the case of heat exchange the specific humidity, q, has to be replaced by the potential temperature, Θ (or the temperature T), where the stomatal resistance, r_{st}, is not considered

The downward shortwave and longwave radiative fluxes $R_{S,f}$ und $R_{L,f}$ can be taken either from monitoring stations of a network or from simple parameterization schemes (e.g., Phillipps, 1962) or more sophisticated radiative transfer models (e.g., Zdunkowski et al., 1982). The other radiative fluxes can be parameterized according to Deardorff (1978).

The heat and water vapour fluxes are given by (Kramm, 1995; see also Fig. 2)

$$H_f = -\sigma_f c_p \rho \left\{ \frac{1}{r_{mt,f}} (\Theta_\delta - T_f) + \frac{1}{r_{mt,fg}} (T_f - T_g) \right\} \tag{16}$$

$$Q_f = -\sigma_f \rho \left\{ \frac{1}{r_{mt,f}} (q_\delta - q_f) + \frac{1}{r_{mt,fg}} (q_f - q_g) \right\} \tag{17}$$

$$H_g = -c_p \rho \left\{ \frac{1-\sigma_f}{r_{mt,g}} (\Theta_\delta - T_g) + \frac{\sigma_f}{r_{mt,fg}} (T_f - T_g) \right\} \tag{18}$$

$$Q_g = -\rho \left\{ \frac{1-\sigma_f}{r_{mt,g}} (q_\delta - q_g) + \frac{\sigma_f}{r_{mt,fg}} (q_f - q_g) \right\}, \tag{19}$$

where Θ_δ and q_δ are the values of potential temperature and specific humidity at the height δ, and q_f is the specific humidity at the leaf surface. The quantities Θ_δ, q_f, and q_δ can be derived from Fig. 2 using Kirchhoff's laws of the electrostatics (see also Kramm, 1995).

2.2.4 The Soil Model

The soil model, which is used to calculate the fluxes of heat and water within the soil as required by Eqs. (14) and (15), is based on a set of two coupled partial differential equations for the soil temperature, T_s, and the volumetric moisture content, η, given by (Philip and de Vries, 1957; de Vries, 1958)

$$C \frac{\partial T_s}{\partial t} = -\frac{\partial H_s}{\partial z} \tag{20}$$

and

$$\rho_w \frac{\partial \eta}{\partial t} = -\frac{\partial W_s}{\partial z}, \tag{21}$$

where

$$H_s = -(\lambda + L_v \rho_w D_{T,v}) \frac{\partial T_s}{\partial z} - L_v \rho_w D_{\eta,v} \frac{\partial \eta}{\partial z} \tag{22}$$

and

$$W_s = -\rho_w \left((D_{\eta,v} + D_{\eta,1}) \frac{\partial \eta}{\partial z} + D_{T,v} \frac{\partial T_s}{\partial z} + K_w \right) \tag{23}$$

represent the total fluxes of heat and moisture within the soil. Here, ρ_w is the density of liquid water, λ is the thermal conductivity, K_w is the hydraulic conductivity, and $D_{T,v}$, $D_{\eta,v}$ as well as $D_{\eta,1}$ are the soil transfer coefficients. The volumetric heat capacity of the soil is defined by $C = (1-P)\,\rho_s c_s + \eta \rho_w c_w$, where P is the porosity (which is equal to the maximum moisture content, η_s), c_s is the specific heat capacity of the soil in a dry state, ρ_s is the soil density, and c_w is the specific heat capacity of water. Note that the heat capacity of air is negligible.

The thermal conductivity varies over several orders of magnitude as the soil dries out. It can be specified as a function of the soil moisture poten-

tial, ψ, by the empirical formula (McCumber and Pielke, 1981)

$$\lambda = \begin{cases} 419\exp(-(Pf+2.7)), & \text{if } Pf < 5.1 \\ 0.172, & \text{if } Pf > 5.1 \end{cases} \quad (24)$$

with $Pf = {}^{10}\log\psi$. The relationship between ψ and the relative humidity, h, can be expressed by (Edlefsen and Anderson, 1943)

$$h = \exp\left(\frac{g\psi}{R_d T_s}\right), \quad (25)$$

where R_d is the gas constant of water vapour.

The parameters ψ and K_w depend on the volumetric moisture content, the saturation hydraulic conductivity, and the porosity. This dependence can be expressed by (Clapp and Hornberger, 1978)

$$\psi = \psi_s\left(\frac{P}{\eta}\right)^b \quad (26)$$

and

$$K_w = K_{w,s}\left(\frac{\eta}{P}\right)^{2b+3}. \quad (27)$$

Taking these quantities into account, the soil transfer coefficients are given by (de Vries, 1958)

$$D_{T,v} = \alpha v_c D_v (P-\eta)\frac{\rho_d}{\rho_w}\frac{L_v(T_s) - g\psi}{R_d T_s^2} \quad (28)$$

$$D_{\eta,v} = -\alpha v_c D_v b \frac{P-\eta}{\eta}\frac{\rho_d}{\rho_w}\frac{g\psi}{R_d T_s} \quad (29)$$

$$D_{\eta,1} = -\frac{bK_{w,s}\psi_s}{\eta}\left(\frac{\eta}{P}\right)^{b+3}, \quad (30)$$

where $D_v = 5.98\cdot 10^{-8} T_s^{2.3}/p$ (p in hPa) is the molecular diffusivity for water vapour in air, ρ_d is the density of water vapour, α is the torsion factor, and $v_c = (1-q_s)^{-1}$ is a correction factor. Since the specific humidity, q_s, within the soil is small, v_c may be approximated by $v_c \approx 1$.

As pointed out by Sasamori (1970), the total fluxes of heat and moisture can be considered as height-invariant within the uppermost soil layer having a thickness of a few millimetres. Integrating Eqs. (22) and (23) over this constant flux layer, $z_{-1} \leqslant z \leqslant 0$, provides the following approximations:

$$H_s \approx -\frac{1}{|z_{-1}|}((\lambda + \rho_w L_v(T_m) D_{T,v}(T_m))(T_g - T_{-1}) + \rho_w L_v(T_m) D_{\eta,v}(\eta_m)(\eta_g - \eta_{-1})) = \text{const.} \quad (31)$$

$$W_s \approx -\frac{\rho_w}{|z_{-1}|}(D_{\eta,v}(\eta_m)(\eta_g - \eta_{-1}) - \frac{b}{b+3}(\psi_g K_{w,g} - \psi_{-1}K_{w,-1}) + 0.5(K_{w,g} + K_{w,-1})|z_{-1}| + D_{T,v}(T_m)(T_g - T_{-1})) = \text{const.} \quad (32)$$

Here, z_{-1} denotes the height of the uppermost grid level within the soil; $T_{-1}, \eta_{-1}, \psi_{-1}$ and $K_{w,-1}$ are the values of soil temperature, volumetric moisture content, soil moisture potential, and hydraulic conductivity at this level; and T_g, η_g, ψ_g and $K_{w,g}$ are the corresponding values at the Earth's surface. The parameters $L_v(T_m)$, $D_{T,v}(T_m)$ and $D_{\eta,1}(\eta_m)$ are functions of the mean quantities $T_m = 0.5\ (T_g + T_{-1})$ and $\eta_m = 0.5\ (\eta_g + \eta_{-1})$.

The budget equations (13) to (15) reduce to a set of coupled non-linear equations which can be solved iteratively by a Newton-Raphson iteration procedure:

$$\mathbf{S}^{(n+1)} = \mathbf{S}^{(n)} - \mathrm{DF}(\mathbf{S}^{(n)})^{-1}\mathrm{F}(\mathbf{S}^{(n)}) \quad (33)$$

with

$$\mathbf{S} = \begin{Bmatrix} T_f \\ T_g \\ \eta_g \end{Bmatrix} \quad (34)$$

and

$$\mathrm{F}(\mathbf{S}) = \begin{Bmatrix} F_1(\mathbf{S}) \\ F_2(\mathbf{S}) \\ F_3(\mathbf{S}) \end{Bmatrix}. \quad (35)$$

Here, DF(**S**) is the functional matrix and $\mathrm{DF}(\mathbf{S})^{-1}$ is the corresponding inverse matrix. The elements of DF(**S**) may be calculated numerically (Kramm, 1995). The degree of accuracy for numerically solving the energy and moisture budget equations (i.e., Eqs. (13) to (15) and (33) to (35)) is determined by $|F_1| < 0.1\ \mathrm{W\,m^{-2}}$, $|F_2| < 0.1\ \mathrm{W\,m^{-2}}$, and $|F_3| < 10^{-7}$, and is usually achieved after five to six iteration steps.

2.3 Kinetic Equations and Transfer Relations

2.3.1 The Reaction Scheme

Nitrogen dioxide predominantly occurs in the troposphere as a result of the oxidation of NO, which is mainly released in combustion processes. Its photodissociation by sunlight ($\lambda < 430$ nm,

e.g., Finlayson-Pitts and Pitts, 1986) leads to the formation of O_3 via collision between an $O(^3P)$ atom and an O_2 molecule, where an N_2 or O_2 molecule usually serves as a third body. Ozone rapidly reacts with NO to regenerate NO_2 so that in the absence of transfer processes and other chemical reactions a photostationary state between NO, NO_2, and O_3 can be achieved. This simple reaction scheme can be summarized by (e.g., Finlayson-Pitts and Pitts, 1986)

$$NO_2 + h\nu \xrightarrow{O_2} NO + O_3 \quad k_1 = \text{variable} \qquad \text{(R1)}$$

$$NO + O_3 \longrightarrow NO_2 + O_2$$
$$k_2 = 1.8 \cdot 10^{-12} \exp(-1370\,K/T), \qquad \text{(R2)}$$

where T is the air temperature in K. The photolysis frequency k_1 is calculated as described by Kramm et al. (1991). The value of k_2 (expressed in cm^3 molecule^{-1} s^{-1}) is taken from Baulch et al. (1984).

The reaction scheme (R1) and (R2) ignores many chemical reactions involved in the photochemical smog formation. To consider a complex chemical mechanism for estimating dry deposition fluxes, the concentrations of about 20 to 25 trace gases would have to be known within the atmospheric surface layer. Such measurements have not been carried out so far. Therefore, our model calculations are restricted to the reactions (R1) and (R2). Even though the formation of HNO_3 can also be addressed (Kramm et al., 1991), it is neglected here to illustrate the way in which our SVAT scheme can be used to estimate dry deposition or emission fluxes of NO, NO_2, and O_3.

2.3.2 Budget Equations and the Modified Profile Scheme

Assuming horizontal homogeneity where advection and horizontal flux divergence are neglected, the following set of coupled non-linear partial differential equations can be derived for the $NO—NO_2—O_3$ triad (e.g., Lenschow, 1982)

$$\frac{\partial [NO_2]}{\partial t} = -\frac{\partial F_{NO_2}}{\partial z} - k_1 [NO_2] + k_2 [NO][O_3] \qquad (36)$$

$$\frac{\partial [NO]}{\partial t} = -\frac{\partial F_{NO}}{\partial z} + k_1 [NO_2] - k_2 [NO][O_3] \qquad (37)$$

$$\frac{\partial [O_3]}{\partial t} = -\frac{\partial F_{O_3}}{\partial z} + k_1 [NO_2] - k_2 [NO][O_3] \qquad (38)$$

where [..] denotes the mean concentrations, and t the time. The reaction rate constant k_2 in Eqs. (36) to (38) may be considered as $k_2 = k_{0,2}(1 + I_s)$, where $k_{0,2}$ is the reaction rate constant experimentally derived within a reactor, and $I_s = <\{NO\}'\{O_3\}'>/([NO][O_3])$ $(-1 \leqslant I_s \leqslant 0)$ is the intensity of segregation (e.g., Lenschow, 1982) which may play an important role in turbulent plumes of reacting species (e.g., Georgopoulos and Seinfeld 1986). The quantities $\{NO\}'$ and $\{O_3\}'$ are the fluctuating deviations from the respective mean concentrations, and $\langle \ldots \rangle$ represents the average. Obviously, the intensity of segregation would lead to a decrease of the 'true' reaction rate constant and, hence, to a decrease of the NO_2 production rate (Vila-Guerau de Arellano and Duynkerke, 1993).

To estimate the influence of the intensity of segregation, it is useful to know whether the reaction (R2) is either kinetically limited ($k_2 \approx k_{0,2}$) or diffusion limited ($k_2 \leqslant k_{0,2}$). The Damköhler number, N_d, is a measure of the ratio of the characteristic diffusion time to the characteristic chemical reaction time for a given reaction. McRae et al. (1982) define those reactions with $N_d > 50$ to be diffusion limited and those with $N_d < 0.01$ to be kinetically limited. Introducing a turbulent Damköhler number for the reaction (R2) by (Stockwell, 1995)

$$N_{d,t} = \frac{k_{0,2}([NO] + [O_3])l^2}{2K_h}, \qquad (39)$$

where l is the mixing length, provides a value of $N_{d,t} < 0.08$ for neutral stratification and a reference height of $z_R = 10$ m as well as moderate mean concentrations of O_3 and NO. Hence, the reaction (R2) tends to be kinetically limited, and k_2 is assumed to be $K_{0,2}$.

Equations (36) to (38) can be rearranged to provide the following budget equation system:

$$\frac{\partial c_j}{\partial t} = -\frac{\partial F_j}{\partial z} \qquad (40)$$

with

$$c_j = \begin{cases} [NO_x] = [NO] + [NO_2] & \text{for } j = 1 \\ [O_x] = [NO_2] + [O_3] & \text{for } j = 2 \\ [NO_x] - [O_x] = [NO] - [O_3] & \text{for } j = 3 \end{cases} \qquad (41)$$

and (with respect to Eq. (2)),

$$F_j = \begin{cases} -D_{NO_2}\dfrac{\partial[NO_2]}{\partial z} - D_{NO}\dfrac{\partial[NO]}{\partial z} - K_h\dfrac{\partial[NO_x]}{\partial z} & \text{for } j=1 \\ -D_{NO_2}\dfrac{\partial[NO_2]}{\partial z} - D_{O_3}\dfrac{\partial[O_3]}{\partial z} - K_h\dfrac{\partial[O_x]}{\partial z} & \text{for } j=2 \\ -D_{NO}\dfrac{\partial[NO]}{\partial z} + D_{O_3}\dfrac{\partial[O_3]}{\partial z} - K_h\dfrac{\partial([NO_x]-[O_x])}{\partial z} & \text{for } j=3 \end{cases} \quad (42)$$

which no longer contains the chemical reactions (R1) to (R2) and, thus, describes the physical behaviour of chemically conservative trace gases. As shown in Eq. (40), the flux F_j of the 'group' concentration c_j will be independent of height if (quasi-) steady state conditions exist during the measurement interval. Thus, Eqs. (3) and (12) are assumed to be valid for estimating such height-invariant fluxes. This may be true for c_2 because the Schmidt numbers and the Henry's law constants of NO_2 and O_3 closely agree so that common values for $r_{mt,i}$, $r_{st,i}$, and $r_{\mathrm{int},i}$ could be considered in the case if both trace species are simultaneously deposited. However, the Schmidt number and the Henry's law constant of NO differ from those of NO_2 and O_3. Furthermore, emission and uptake of these nitrogen species can occur at the same site on separate occasions (e.g., emission of NO and deposition of NO_2). Thus, it seems to be doubtful that the common use of any resistances depending on the characteristics of the 'individual' trace gases (which would lead to commonly used deposition and emission velocities) provides reasonable results. Moreover, environmental impact research requires a quantitative determination of the uptake of the 'individual' trace species, rather than that of the combinations mentioned above. Therefore, combined fluxes have to be separated to their 'individual' trace species and the chemical reactions among NO, NO_2, and O_3 would have to be considered. Since, however, the relation between chemical transformation and transport processes within the canopy and the uptake or emission effects are highly complex, in the present study chemical reactions are considered only within the fully turbulent part of the atmospheric surface layer. Hence, a flux resistance relationship for the molecular-turbulent sublayer and the canopy layer given by (Kramm, 1991)

$$F_i = -\frac{c_{\delta,i}}{r_{mt,i}+r_{s,i}}(1-\mu_i) = \text{const.} \quad (43)$$

is used. Here, the subscript i stands for NO, NO_2, or O_3.

The turbulent flux, for example, of O_3 can be calculated on the basis of a set of coupled nonlinear ordinary differential equations, given by (Kramm, 1989)

$$\frac{\partial F_{O_3}}{\partial z} = k_1 c_2 - (k_1 + k_2 c_3)[O_3] - k_2[O_3]^2 \quad (44)$$

$$\frac{\partial[O_3]}{\partial z} = -\frac{F_{O_3}}{K_h}. \quad (45)$$

This two-point boundary-value problem may numerically be solved with the shooting method and with reference to Gear's (1971) backward differentiation formulae.

Routine data of wind speed, temperature, humidity and concentrations of NO, NO_2, and O_3 serve as upper boundary conditions at the height z_R. The lower boundary conditions, i.e., the concentrations of the 'individual' trace species at the height δ and the 'group' concentrations c_1, c_2, and c_3 at the same height have to be calculated simultaneously. Here, the calculations of the lower boundary conditions are based on the requirement that the flux divergences $\partial F_{NO}/\partial z$, $\partial F_{NO_2}/\partial z$, and $\partial F_{O_3}/\partial z$ vanish at the height δ so that the right side of Eq. (44) can be considered as equal to zero. This leads to the chemical equilibrium between NO, NO_2, and O_3. The requirement is a consequence of the constant flux approximation expressed in Eq. (43) on which the resistance approach for the molecular-turbulent sublayer and the canopy layer is based even in the case of chemically reactive trace species. This approximation agrees with that used in enclosure techniques for determining the canopy and molecular-turbulent resistances. The calculation of the lower

boundary conditions can only be carried out iteratively (see Kramm and Dlugi, 1994; Kramm, 1995). When the lower boundary conditions have been determined, equation set (44) and (45) can be solved. The 'group' concentrations c_1, c_2, and c_3 can be calculated along with the eddy diffusivity K_h for each level $\delta \leqslant z \leqslant z_R$.

3. Model Tests and Preliminary Results

Data of wind speed, temperature, humidity and concentrations averaged over a certain period are employed to numerically determine the vertical fluxes of momentum, sensible and latent heat, NO, NO_2, and O_3. Unfortunately, at present only a few data sets of these mean quantities exist which allow testing of our SVAT scheme. Moreover, the evaluation of our model on the basis of the trace gas fluxes and the corresponding fluxes of momentum, sensible and latent heat simultaneously measured during the SANA field campaign SADE '94 by eddy correlation techniques at two heights (Beier et al., 1995) has to be postponed until the results of these flux measurements are available.

Vertical fluxes of momentum, sensible and latent heat as well as NO, NO_2, and O_3 were determined on the basis of wind speed, dry-bulb temperature, specific humidity, and the concentrations of these trace gases measured by the Institute of Atmospheric Chemistry III at the Forschungszentrum (KFA) Jülich at heights of 0.40, 2.60 and 17.20 m above an even terrain, covered with sugar beet (25 cm tall), near Jülich in western Germany in September 1984 (Höfken et al., 1986). Wind speed and temperature data were averaged over 5 min. Concentrations of NO and NO_2 (2 min averages) were determined by chemiluminescent techniques applying a modified commercial $NO/NO_2/NO_x$ analyser (Thermo Electron 14 A) with a detection limit of 0.1 ppb. An UV absorption method (Dasibi 1003-AH, 1 ppb detection limit) was used to measure the O_3 concentration (2 min averages). These data were also used by Kramm (1989) and Kramm et al. (1991) to compute the vertical profiles of wind speed, temperature, humidity and concentrations and the corresponding turbulent fluxes (see Figs. 3 and 4). In contrast to those calculations, in the present study only the data observed at the 17.2 m level are used. Neither soil temperature and soil moisture nor compensation point concentrations were measured under field conditions. Moreover, the determination of σ_f and the plant-specific

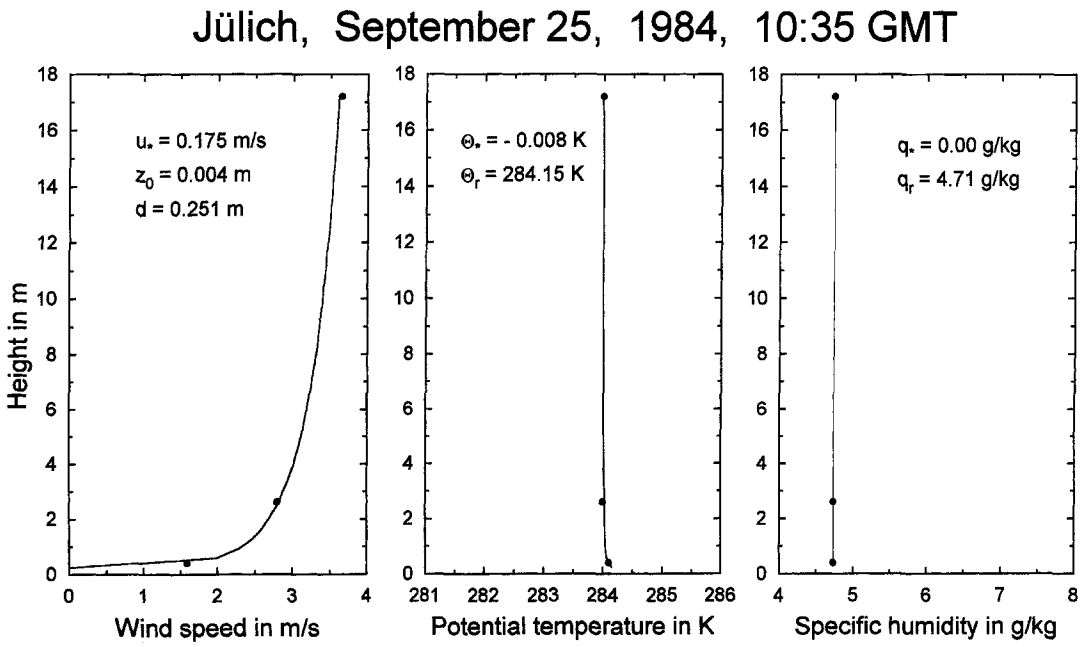

Fig. 3. Vertical profiles of wind speed, potential temperature and specific humidity. The solid symbols represent the measured values (Höfken et al., 1986), and the lines the calculated vertical profiles (Kramm et al., 1991)

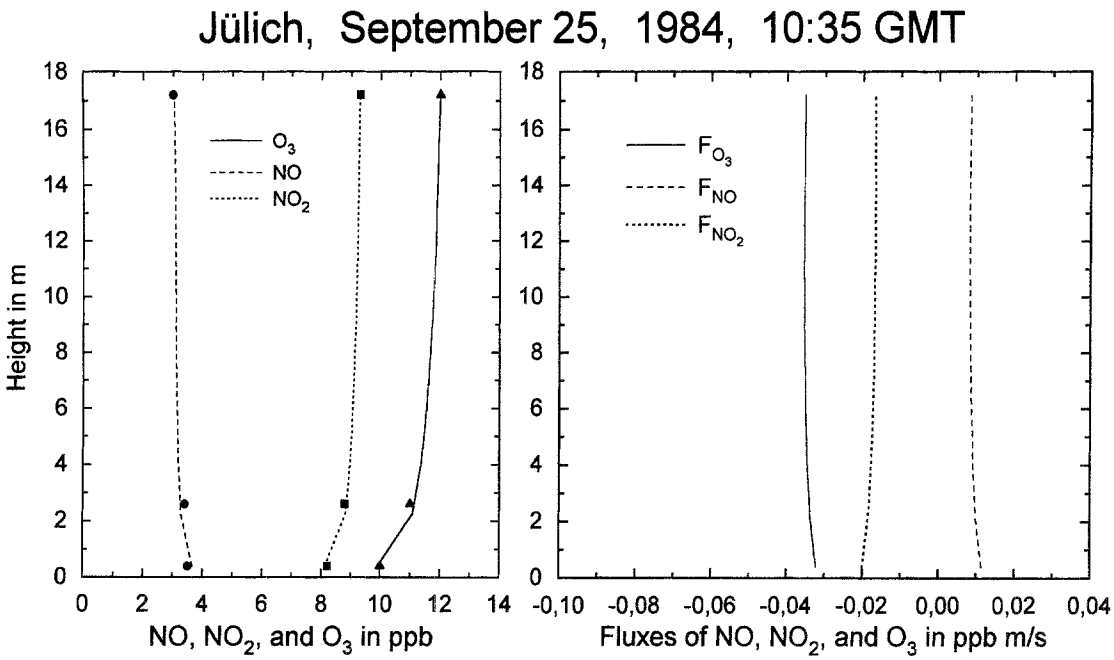

Fig. 4. As in Fig. 3, but for concentrations and turbulent fluxes of NO, NO_2, and O_3

Table 1. *Input Data used for Model Tests*

Atmosphere:

z (m)	U (m/s)	Θ (K)	q (g/kg)	NO (ppb)	NO_2 (ppb)	O_3 (ppb)
17.2	3.65	283.99	4.73	3.0	9.3	12.0

$R_{s,f}\downarrow = 165\ \mathrm{W/m^2}$ (estimated), $z_0 = 0.004$ m, $d = 0.251$ m

Soil (arbitrarily chosen):

z_{-1} (m)	T_{-1} (K)	η_{-1}	P	$K_{w,s}$ (m/s)	ψ_s (m)	b
−0.025	281.0	0.2	0.435	$3.4\cdot10^{-5}$	−0.218	4.9

Vegetation (arbitrarily chosen):

$r_{st,min}$ (s/m)	b_{st} (W/m²)	T_{min} (°C)	T_{max} (°C)	T_{opt} (°C)
65	10	5	45	25

parameters as required in Jarvis's formulae (see Eq. (11) and Appendix A) could not be carried out, and adequate values were not found in the literature. Therefore, the values of soil temperature and soil moisture as well as plant-specific quantities were chosen arbitrarily. The input data used in our study are listed in Table 1.

Figure 5 shows results for the vertical profiles of wind speed, temperature and humidity provided by the SVAT scheme. These results were derived for different values of σ_f ranging from $\sigma_f = 1$ (i.e., the soil is totally covered by vegetation) to $\sigma_f = 1/7$ (i.e., nearly bare soil). They indicate that the thermal stratification varies from slightly unstable to stable when σ_f decreases. Figure 6 shows the influence of σ_f upon the sensible and latent heat fluxes above the vegetation and between the foliage and the soil as well as the soil heat flux.

Compared with the results shown in Fig. 3, only the results derived for a soil surface totally covered by vegetation ($\sigma_f = 1$) seem to be adequate for the input values that were arbitrarily chosen (Table 1). Therefore, only the results of the vertical fluxes of NO, NO_2, and O_3 derived for $\sigma_f = 1$ are discussed.

The results illustrated in Fig. 4 suggest that in the case of the Jülich data the turbulent fluxes of NO, NO_2, and O_3 are nearly height-invariant. Since the concentrations of NO, NO_2, and O_3 at the heights of 0.4 m, 2.6 m and 17.2 together with the NO_2 photolysis frequency, $k_1 = 0.087\ \mathrm{min^{-1}}$ (cloud cover = 8/8), and the reaction rate constant $k_2 = 22.1\ \mathrm{ppm^{-1}\ min^{-1}}$ indicate a photostationary state characterized by the Leighton relationship, the calculation of the turbulent fluxes of these trace species has to provide height-invariant

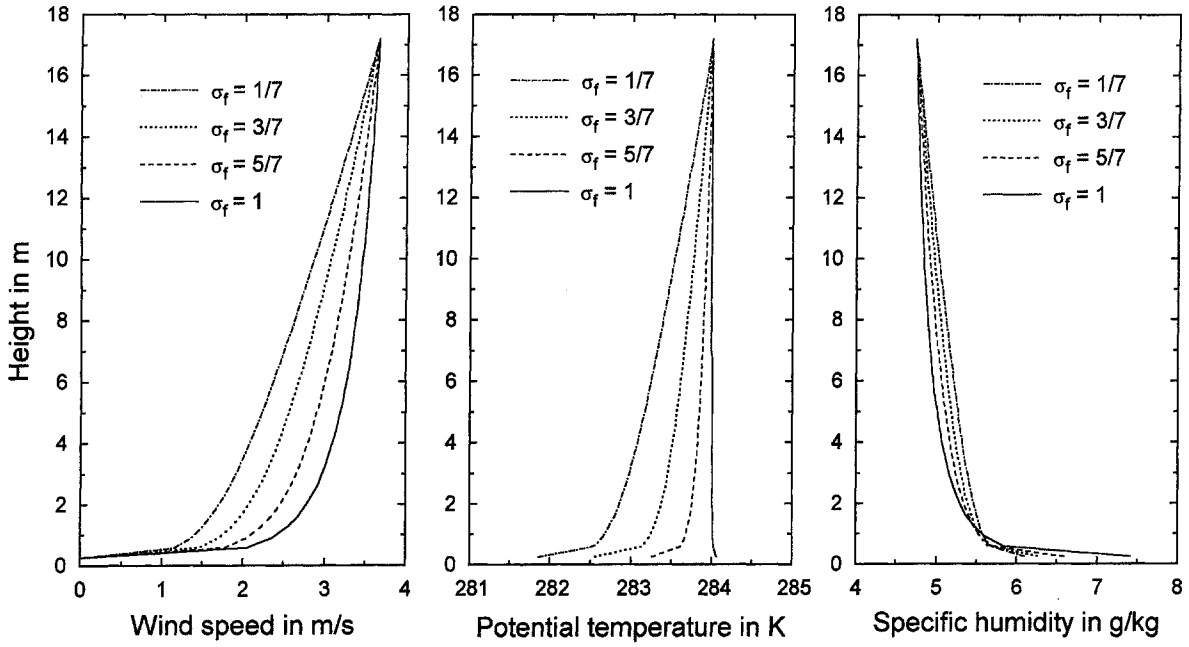

Fig. 5. Vertical profiles of wind speed, potential temperature and specific humidity calculated for different values of the shielding factor, σ_f

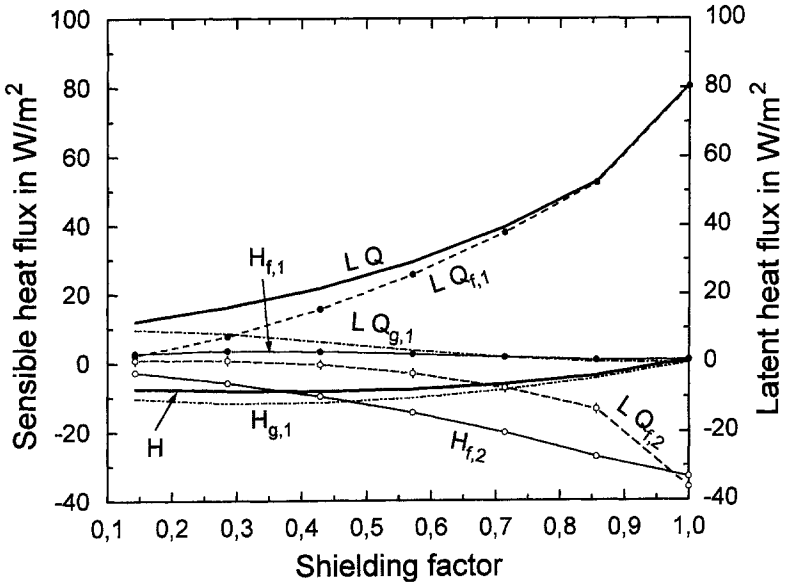

Fig. 6. Plot of the fluxes of sensible and latent heat vs. shielding factor, σ_f. Here, H and $L\,Q$ are the turbulent fluxes above vegetationen, $H_{f,1}$ and $L\,Q_{f,1}$ are the fluxes between the foliage and the height δ, $H_{g,1}$ and $L\,Q_{g,1}$ are the fluxes between the bare soil surface and the same height, and $H_{f,2}$ and $L\,Q_{f,2}$ are the fluxes between the foliage and the soil surface

fluxes, even if chemical reactions are included. Although the influence of chemical reactions on dry deposition (or emission) fluxes of NO, NO_2, and O_3 cannot be well demonstrated on the basis of these data, we have, nevertheless, used these data due to the lack of better data at present.

Test results of sensitivity studies regarding deposition and emission of NO and NO_2 are illustrated in Figs. 7 and 9. Arbitrary values of $c_{sl,NO}$, ranging from zero to 35 ppb, and c_{sl,NO_2} ranging from zero to 12 ppb, were used to switch from deposition to emission or vice versa (see also Table 3), where substrate concentrations of O_3 were neglected. The sensitivity studies were performed for a nearly dry foliage surface. Typical results of the calculated values of the molecular-turbulent resistances and the substrate resistances are listed in Table 2.

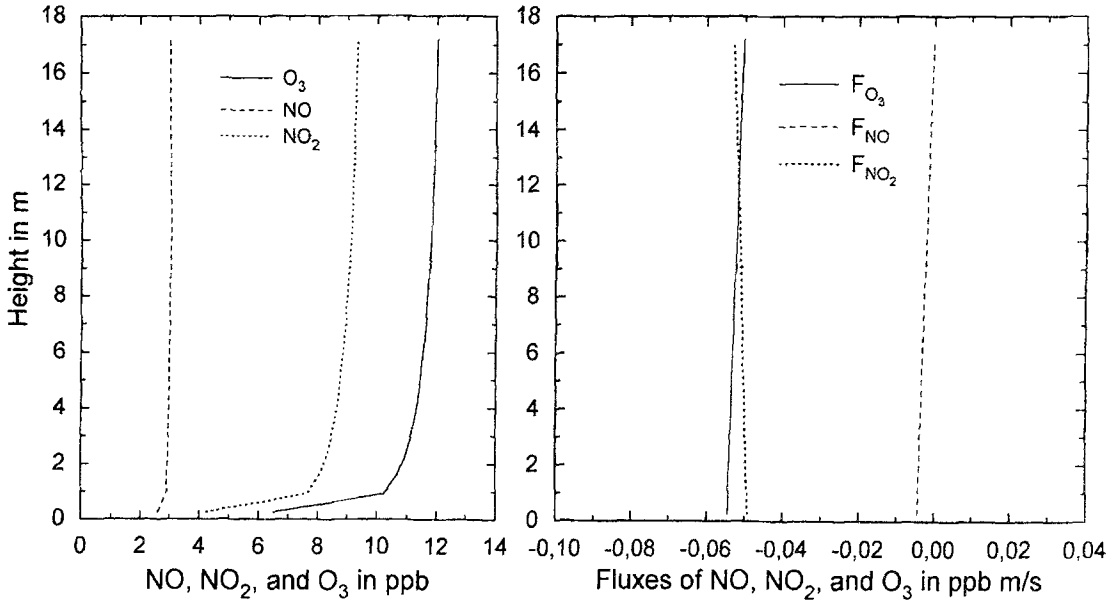

Fig. 7. Vertical profiles of concentrations and turbulent fluxes of NO, NO_2, and O_3 for $c_{sl,NO} = c_{sl,NO_2} = 0$

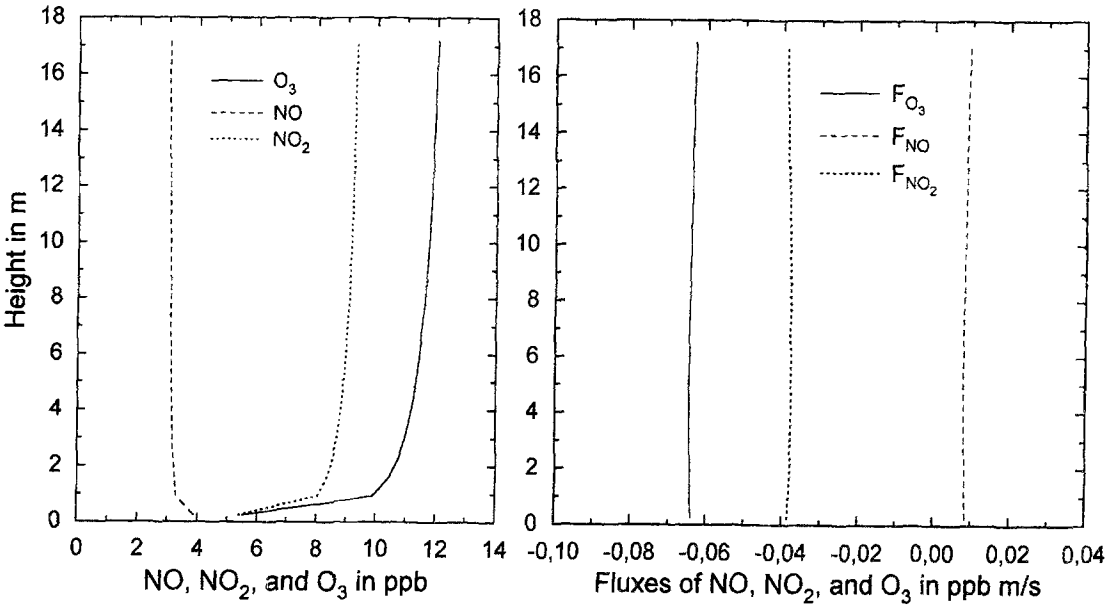

Fig. 8. As in Fig. 7, but for $c_{sl,NO} = 22$ ppb, $c_{sl,NO_2} = 12$ ppb

Figure 7 illustrates that in the case of $c_{sl,NO} = c_{sl,NO2} = 0$ (maximum deposition) the fluxes of NO, NO_2, and O_3 considerably differ from those shown in Fig. 4. The same is true in the case of increasing $c_{sl,NO}$ values ($c_{sl,NO_2} = 0$). The shapes of the vertical flux profiles are similar for all states, where especially the deposition fluxes of NO and NO_2 decrease. The vertical concentration profiles are nearly identical except close to the ground, where the profile values show small differences. The compensation point concentration of NO amounts to about 9 ppb. Similar results can be obtained for increasing c_{sl,NO_2} values ($c_{sl,NO} = 0$), but in this case a compensation point concentration could not be determined.

Since the results of these sensitivity studies did not agree with those of Fig. 4, further attempts with different soil concentrations of NO and NO_2

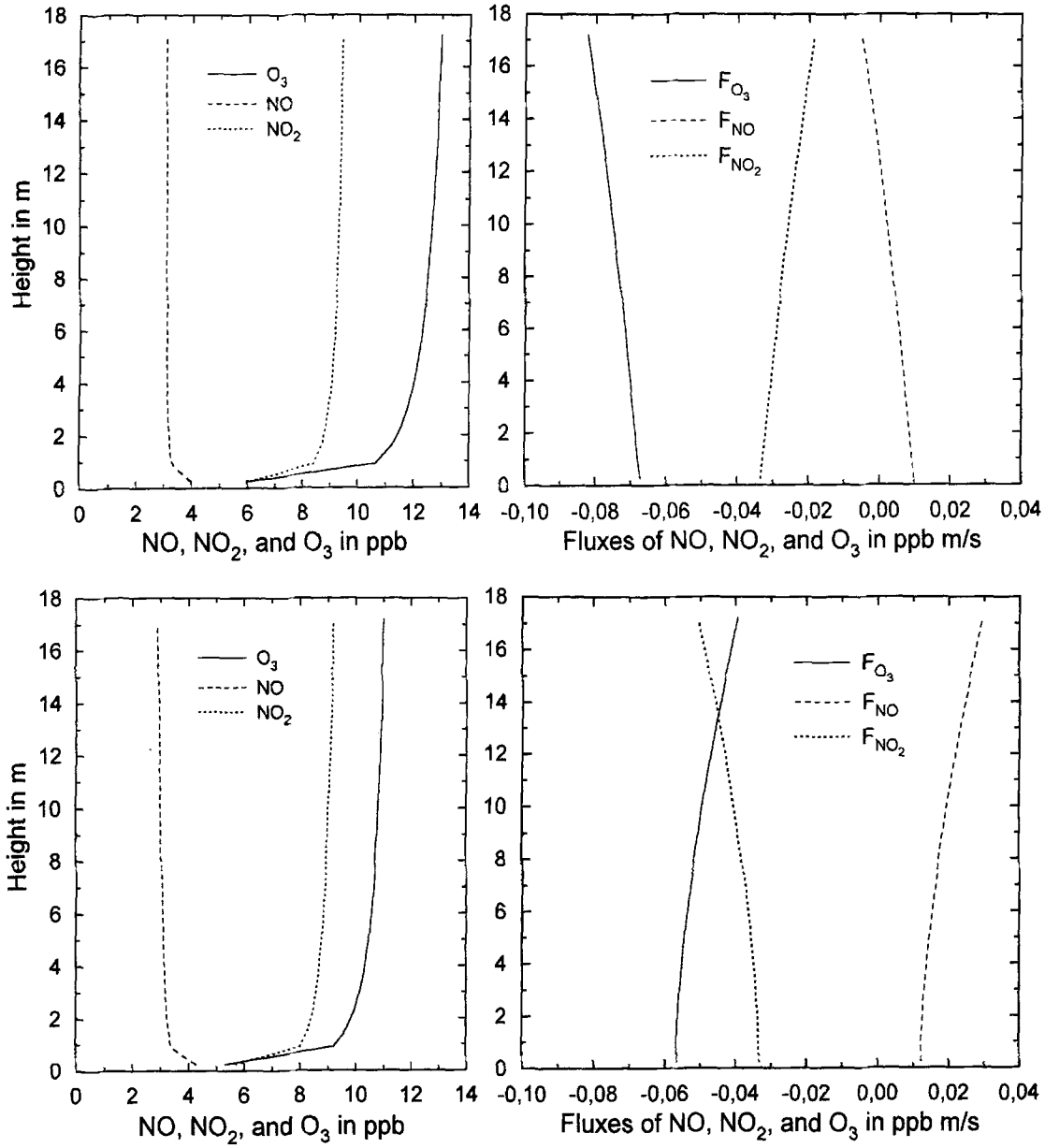

Fig. 9. As in Fig. 8, but for concentrations arbitrarily altered by ± 100 ppt (NO and NO_2) and ± 1 ppb (O_3)

both greater than zero were made to achieve a better agreement. In comparison with the results shown in Fig. 4 the "best" agreement was obtained for $c_{s1,NO} = 22$ ppb and $c_{s1,NO2} = 12$ ppb (see Fig. 8), where, however, the deposition fluxes of NO_2 and O_3 are more than 50% larger as indicated in Fig. 4. Seemingly, a better agreement can be achieved if measurements of soil-specific concentrations (dependent on soil temperature and soil moisture) and plant-specific parameters are available. Therefore, these quantities should concurrently be determined with the eddy fluxes of trace gases, momentum, sensible and latent heat as well as the vertical profiles of concentrations, wind speed, temperature and humidity in future field experiments designed for model evaluation.

Usually, the incoming solar radiation or the photolysis frequency of NO_2, k_1, can be measured with a sufficient degree of accuracy. Furthermore, the value of the reaction rate constant k_2 is widely accepted so that the accuracy of the calculated flux profiles may be sufficient (discrepancies in the results when the k_2 value is changed were already

Table 2. *Calculated Resistances for* NO, NO_2, *and* O_3. *Note that the Values of* $r_{sl,i} = 500\,s\,m^{-1}$ *and* $r_{w,i} = 500\,s\,m^{-1}$ *were Arbitrarily chosen. Furthermore, the Value* μ_{NO} *corresponds to a Substrate Concentration of* $c_{sl,NO} = 5$ *ppb*

	NO	NO_2	O_3
	Resistances is $s\,m^{-1}$-Units		
$r_{st,i}^{\alpha}$	167.5	206.1	206.1
$H_i \cdot r_{int,i}^{\beta}$	9400.0	500.0	500.0
$r_{cu,i}$	2152.5	2649.5	2649.5
$r_{s,i}$	178.0	72.7	72.7
$r_{mt,i}$	27.2	31.2	31.2
$r_{mt,fg,i}^{\gamma}$	82.1	96.9	96.9
μ_i	0.63	0.0	0.0
H_i	22.6	4.3	4.6
Sc_i	0.72	0.88	0.88

$^{\alpha}$ According to Jarvis (1976), Eqs. (11) of the present study.
$^{\beta}$ Values of NO and NO_2 taken from O'Dell et al. (1977), the O_3 value corresponds to that of NO_2.
$^{\gamma}$ According to Eq. (7) of our study.

Table 3. *Results of the Ozone Fluxes,* $F_{O_3,mt}$ *and* $F_{O_3,t}$, *calculated for the Lower Boundary* δ

Case	$c_{sl,NO}$ (ppb)	c_{sl,NO_2} (ppb)	$F_{O_3,mt}$ (ppb m/s)	$F_{O_3,t}$ (ppb m/s)
1	0	0	−0.063	−0.055
2	5	0	−0.060	−0.057
3	9	0	−0.058	−0.059
4	12	0	−0.057	−0.060
5	0	5	−0.064	−0.054
6	0	9	−0.064	−0.053
7	12	12	−0.059	−0.058
8	22	12	−0.055	−0.062
9[α]	0	0	−0.060	−0.048
10[α]	22	12	−0.052	−0.056

$^{\alpha}$ Upper boundary conditions were altered (see text).

discussed by Kramm et al., 1991). However, uncertainties in the flux profiles may also be affected by a small displacement in the concentrations of NO, NO_2, and O_3. Such a displacement can be substantiated by the detection limits of chemical sensors.

To investigate this aspect in the vicinity of a photostationary state as considered here, the concentration values of NO and NO_2 were arbitrarily altered by 100 ppt and the concentration value of O_3 by 1 ppb. Results derived for the soil concentrations $c_{sl,NO} = 22$ ppb and $c_{sl,NO_2} = 12$ ppb are illustrated in Fig. 9. As expected, these results indicate that in the vicinity of the photostationary state a small displacement in the concentrations of NO, NO_2, and O_3 can produce large discrepancies in the flux results, which are manifested here by the shift from height-invariant fluxes substantiated by the photostationary state to strongly height-dependent fluxes realized by the departure from that state. Since the alteration of the O_3 concentration mainly contributes to these discrepancies in the flux results, the accuracy with which this concentration can be measured has to be improved to derive reliable flux estimates.

To calculate the lower boundary conditions at the outer edge of the molecular-turbulent sublayer, the requirement that the flux divergences $\partial F_{NO}/\partial z$, $\partial F_{NO_2}/\partial z$, and $\partial F_{O_3}\partial/z$ vanish at the height δ was introduced which leads to the chemical equilibrium between NO, NO_2, and O_3. This requirement is a consequence of the constant flux approximation expressed in Eq. (43) on which the resistance approach for the molecular-turbulent sublayer and the canopy layer is based. Although the theoretical concept is formulated in a consistent manner, there are still some problems in matching the fluxes at the height δ (see also Kramm and Dlugi, 1994). Typical flux results obtained by the flux-resistance relationship for the molecular-turbulent sublayer and the canopy layer, $F_{O_3,mt}$, and those derived for the turbulent region using the shooting method, $F_{O_3,t}$ are listed in Table 3. This table indicates differences between these two fluxes as large as 20%. It seems that these differences are produced by the small amounts of the eddy diffusivity at the outer edge of the molecular turbulent sublayer. Since the flux-resistance relationship and the eddy diffusivity are used to derive the start values for the shooting method, the small amount of the eddy diffusivity can produce large discrepancies between the concentrations of NO, NO_2, and O_3 and the corresponding calculated concentrations at the upper boundary z_R. Thus, the shooting

method requires a new iteration step and, hence, the flux amount calculated for the lower boundary, δ, differs from that derived by the flux-resistance relationship (43). Therefore, the requirement mentioned above as well as the matching of the fluxes demand further investigations. This includes, of course, the parameterization of the transfer of matter and heat across the molecular-turbulent sublayer when highly reactive trace gases are considered.

4. Summary and Conclusions

A SVAT scheme for determining the dry deposition and/or emission fluxes of NO, NO_2, and O_3 in the atmospheric surface layer over horizontally uniform terrain covered with fibrous canopy elements was presented and discussed. Its preliminary results suggest that these dry deposition fluxes are not only influenced by meteorological and plant-physiological parameters, but also by chemical reactions among these trace species as well as NO emission from the soil. A small displacement in the concentrations of NO, NO_2, and O_3 within the range of the detection limits of the chemical sensors, for instance, can produce large discrepancies in the flux estimates which are manifested here by the shift from height-invariant to strongly height-dependent fluxes. Consequently, (a) the relatively large detection limit of O_3 analysers has to be reduced to derive reliable flux estimates, and (b) the widely used 'big leaf' multiple resistance approach, which is based on the constant flux approximation, seems to be inappropriate for computing dry deposition fluxes and deposition velocities of NO and NO_2.

Obviously, final evaluation of the model presented here must be postponed until the fluxes of these species directly measured together with those of momentum, sensible and latent heat during the SADE '94 campaign by eddy correlation techniques at two heights (Beier et al., 1995) are finally evaluated.

Acknowledgements

We would like to express our thanks to the Bundesminister für Forschung und Technologie (BMFT), contracts SANA B 3.5 (Sanierung der Atmosphäre über den neuen Bundesländern) and 07EU745 3, EUROTRAC-Subproject BIATEX, for support of this contribution. Thanks also to Dr. Nicole Mölders from the Unversity of Leipzig and Dr. William R. Stockwell from IFU for helpful comments.

Appendix A

Following Jarvis (1976) and Hicks et al. (1987), the correction functions can be expressed by

$$g_\delta(\delta_e) = 1 - b_e \delta_e, \tag{A1}$$

$$g_\psi(\psi) = \begin{cases} 1, & \text{if } \psi > \psi_t \\ a_\psi \psi + b_\psi, & \text{if } \psi \leqslant \psi_t, \end{cases} \tag{A2}$$

$$g_T(T_f) = \frac{T_f - T_{\min}}{T_{\text{opt}} - T_{\min}} \left[\frac{T_{\max} - T_f}{T_{\max} - T_{\text{opt}}} \right]^{b_T} \tag{A3}$$

with

$$b_T = \frac{T_{\max} - T_{\text{opt}}}{T_{\text{opt}} - T_{\min}}, \tag{A4}$$

and

$$g_c(CO_2) = \begin{cases} 1, & \text{if } [CO_2] \leqslant 100 \\ 1 - b_{C1}[CO_2], & \text{if } 100 < [CO_2] < 1000 \\ b_{C2}, & \text{if } [CO_2] > 1000. \end{cases} \tag{A5}$$

Here, $\delta_e = e_s(T) - e$ is the water vapour deficit (where $e_s(T)$ is the saturated water vapour pressure at air temperature T, and e is the ambient water vapour pressure), ψ is the leaf water potential, ψ_t is a species-dependent threshold value, T_f is the temperature of the foliage, $[CO_2]$ is the ambient CO_2 concentration in ppmv, $T_{\min}$ and $T_{\max}$ are species-dependent higher and lower temperature extremes at which stomata no longer open, respectively. The quantity T_{opt} is the temperature at which stomatal exchange is optimized. The quantities b_e, a_ψ, b_ψ, b_{C1}, and b_{C2} are empirical constants dependent on the plant species. Values for $r_{st,\min}$, b_{st}, $T_{\min}$, and T_{opt}, for instance, are given by Jarvis (1976), Körner et al. (1979), Hicks et al. (1987), and Baldocchi et al. (1987). Note that $g_C(CO_2) = 1$ was arbitrarily chosen for our model studies.

References

Allen, L. H., Lemon, E. R., 1972: Net radiation frequency distribution in a corn crop. *Bound.-Layer Meteor.*, **3**, 246–254.

Baldocchi, D. D., Hicks, B. B., Camara, P., 1987: A canopy stomatal resistance model for gaseous deposition to vegetated surfaces. *Atmos. Environ.*, **21**, 91–101.

Baldocchi, D. D., 1988: A multi-layer model for estimating sulfur dioxide deposition to a deciduous oak forest canopy. *Atmos. Environ.*, **22**, 869–884.

Baldocchi, D. D., Hicks, B. B., Meyers, T. P., 1988: Measuring biosphere-atmosphere exchanges of biologically related gases with micrometeorological methods. *Ecology*, **69**, 1331–1340.

Baulch, D. L., Cox, R. A., Hampson, Jr., R. F., Kerr, J. A., Troe, J., Watson, R. T., 1984: Evaluated kinetic and photochemical data for atmospheric chemistry: Supplement II. *J. Phys. Chem. Ref. Data*, **13**(4), 1259–1380.

Beier, N., Schroers, H., Müller, D., Weber, M., 1995: Grenzschichtuntersuchungen zur trockenen Deposition inerter und reaktiver Spurenstoffe. BMFT-Verbundforschungsprojekt SANA, Jahresbericht 1994, IFU, Garmisch-Partenkirchen (in German).

Beljaars, A. C. M., Holtslag, A. A., 1991: Flux parameterization over land surfaces for atmospheric models. *J. Appl. Meteor.*, **30**, 327–341.

Brutsaert, H. W., 1975: The roughness length for water vapor, sensible heat, and other scalars. *J. Atmos. Sci.*, **32**, 2028–2031.

Businger, J. A., 1986: Evaluation of the accuracy with which dry deposition can be measured with current micrometeorological techniques. *J. Appl. Meteor.*, **25**, 1100–1124.

Chamberlain, A. C., 1968: Transport of gases to and from surfaces with bluff and wave-like roughness elements. *Quart. J. Roy. Meteor. Soc.*, **94**, 318–332.

Chang, J. S., Brost, R. A., Isaksen, I. S. A., Madronich, S., Middleton, P., Stockwell, W. R., Walcek, C. J., 1987: A three-dimensional Eulerian acid deposition model: Physical concepts and formulation. *J. Geophys. Res.*, **92**, 14681–14700.

Clapp, R., Hornberger, G., 1978: Empirical equations for some soil hydraulic properties. *Water Resour. Res.*, **14**, 601–604.

Deacon, E. L., 1977: Gas transfer to and across an air-water interface. *Tellus*, **29**, 363–374.

Deardorff, J. W., 1978: Efficient prediction of ground surface temperature and moisture, with inclusion of a layer of vegetation. *J. Geophys. Res.*, **83**(C4), 1889–1903.

Delany, A. C., Fitzjarrald, D. R., Lenschow, D. H., Pearson, Jr., R., Wendel, G. J., Woodruff, B., 1986: Direct measurements of nitrogen oxides and ozone fluxes over grassland. *J. Atmos. Chem.*, **4**, 429–444.

De Vries, D. A., 1958: Simultaneous transfer of heat and moisture in porous media. *Trans. Amer. Geophys. Union*, **39**, 909–916.

Droppo, Jr., J. G., 1985: Concurrent measurements of ozone dry deposition using eddy correlation and profile flux methods. *J. Geophys. Res.*, **90**(D1), 2111–2118.

Dyer, A. J., Hicks, B. B., 1970: Flux-gradient relationships in the constant flux layer. *Quart. J. Roy. Meteor. Soc.*, **96**, 715–721.

Edlefsen, N. E., Anderson, A. B. C., 1943: The thermodynamics of soil moisture. *Hilgardia*, **16**, 31–299.

Finlayson-Pitts, B. J., Pitts, Jr., J. N., 1986: *Atmospheric Chemistry*. Chichester, New York, Brisbane, Toronto, Singapore: J. Wiley, pp. 1098.

Fitzjarrald, D. R., Lenschow, D. H., 1983: Mean concentration and flux profiles for chemically reactive species in the atmospheric surface layer. *Atmos. Environ.*, **17**, 2505–2512.

Gao, W., Wesely, M. L., Lee, I. Y., 1991: A numerical study of the effects of air chemistry on fluxes of NO, NO_2, and O_3 near the surface. *J. Geophys. Res.*, **96**(D10), 18761–18769.

Garratt, J. R., Hicks, B. B., 1973: Momentum, heat and water vapour transfer to and from natural and artificial surfaces. *Quart. J. Roy. Meteor. Soc.*, **99**, 680–687.

Gear, C. W., 1971: *Numerical Initial Value Problems in Ordinary Differential Equations*. Englewood Cliffs, New Jersey: Prentice-Hall, pp. 253.

Georgopoulos, P. G., Seinfeld, J. H., 1986: Mathematical modeling of turbulent reacting plumes-I. General theory and model formulation. *Atmos. Environ.*, **20**, 1791–1807.

Hanson, P. J., Lindberg, S. E., 1991: Dry deposition of reactive nitrogen compounds: A review of leaf, canopy and non-foliar measurements. *Atmos. Environ.*, **25A**, 1615–1634.

Hasse, L., 1971: The sea surface temperature deviation and the heat flow at the sea-air interface. *Bound.-Layer Meteor.*, **1**, 368–379.

Herbert, F., 1987: Mechanismen der nassen und trockenen Deposition. In: Jaenicke, R. (ed.) *Atmosphärische Spurenstoffe*. Weilheim: VCH Verlagsgesellschaft, 241–269 (in German).

Hicks, B. B., 1976: Some micrometeorological aspects of pollutant deposition rates near the surface. In: Engelmann, R. J., Sehmel, G. A. (eds.) *Atmosphere-Surface Exchange of Particulate and Gaseous Pollutants (1974)*. Techn. Inf. Center, Office of Public Affairs, ERDA, Oak Ridge, TN., U.S.A., 434–449.

Hicks, B. B., Baldocchi, D. D., Meyers, T. P., Hosker, Jr., R. P., Matt. D. R., 1987: A preliminary multiple resistance routine for deriving dry deposition velocities from measured quantities. *Water, Air, and Soil Pollution*, **36**, 311–330.

Hicks, B. B., Matt, D. R., 1988: Combining biology, chemistry, and meteorology in modeling and measuring dry deposition. *J. Atmos. Chem.*, **6**, 117–131.

Höfken, K. D., Meixner, F., Müller, K. P., Ehhalt, D. H., 1986: Untersuchungen zur trockenen Deposition und Emission von atmosphärischem NO, NO_2 und HNO_3 an natürlichen Oberflächen. Berichte der KFA Jülich, No. **2054**, Jülich, F.R.G. (in German).

Högström, U., 1967: Turbulent water vapour transfer at different stability conditions. *Phys. of Fluid*, **10** [Suppl.], 247–254.

Jarvis, P. G., 1976: The interpretation of the variations in leaf water potential and stomatal conductance found in canopies in the field. *Phil. Trans. R. Soc., London, B*, **273**, 593–610.

Körner, Ch., Scheel, J. A., Bauer, H., 1979: Maximum leaf diffusive conductance in vascular plants. *Photosynthetica*, **13**, 45–82.

Kramm, G., Herbert, F., 1984: Ein numerisches Modell zur Deposition von Schadstoffen in der bodennahen Luftschicht. In: Reuter, H. (ed.) *Probleme der Umwelt- und Medizinmeteorologie im Gebirge*. Zentralanstalt f. Meteorologie u. Geodynamik, Wien, Nr. **288**, 22–38, 1984 (in German).

Kramm, G., 1989: A numerical method for determining the dry deposition of atmospheric trace gases. *Bound.-Layer Meteor.*, **48**, 157–176.

Kramm, G., 1991: Numerical investigation of the dry deposition of reactive trace gases. In: Borrell, P., Borrell, P. M., Seiler, W. (eds.) *Transport and Transformation of Pollutants in the Troposphere*. Proc. of EUROTRAC Symposium '90, Garmisch-Partenkirchen, April 2–5, 1990. SPB Academic Publ. bv., The Hague, The Netherlands, 155–157.

Kramm, G., Müller, H., Fowler, D., Höfken, K. D., Meixner, F. X., Schaller, E., 1991: A modified profile method for determining the vertical fluxes of NO, NO_2, ozone, and HNO_3 in the atmospheric surface layer. *J. Atmos. Chem.*, **13**, 265–288.

Kramm, G., Beheng, K.-D., Müller, H., 1992: Vertical transport of polydispersed aerosol particles in the atmospheric surface layer. In: Schwartz, S. E., Slinn, W. G. N., (eds.) *Precipitation Scavenging and Atmosphere-Surface Exchange Processes,* Vol. 2-The Semonin Vol. New York: Hemisphere, pp. 1125–1141.

Kramm, G., Dlugi, R., 1994: Modelling of the vertical fluxes of nitric acid, ammonia, and ammonium nitrate in the atmospheric surface layer. *J. Atmos. Chem.*, **18**, 319–357.

Kramm, G., 1995: Zum Austausch von Ozon und reaktiven Stickstoffverbindungen zwischen Atmosphäre und Biosphäre. Frankfurt/Main: Wissenschafts-Verlag Dr. W. Maraun, pp. 268 (in German).

Kramm, G., Müller, H., Dlugi, R, 1995: On the relationship between the roughness length of a scalar quantity and the corresponding sublayer-Stanton number. *Meteorol. Zeitschrift, NF,* **4**, 209–212.

Lenschow, D. H., 1982: Reactive trace species in the boundary layer from a micrometeorological perspective. *J. Meteor. Soc. Japan,* **60**, 472–480.

Lenschow, D. H., Delany, A. C., 1987: An analytic formulation for NO and NO_2 flux profiles in the atmospheric surface layer. *J. Atmos. Chem.*, **5**, 301–309.

Lenschow, D. H., Hicks, B. B., (eds.) 1989: *Global Tropospheric Chemistry–Chemical Fluxes in the Global Atmosphere.* Boulder, CO: National Center for Atmospheric Research, pp. 107.

McCumber, M. C., Pielke, R. A., 1981: Simulation of the effects of surface fluxes of heat and moisture in a mesoscale numerical model–1. soil layer. *J. Geophys. Res.*, **86**(C10), 9929–9938.

McRae, G. J., Goodin, W. R., Seinfeld, J. H., 1982: Mathematical modeling of photochemical air pollution. *Environmental Quality Laboratory Report No.* **18**, California Institute of Technology, Pasadena, CA.

Monteith, J. L., Szeicz, G., Waggoner, P. E., 1965: The measurement of stomatal resistance in the field. *J. Appl. Ecol.*, **2**, 345–355.

Monteith, J. L., (ed.), 1975: *Vegetation and the Atmosphere, Vol. 1, Principles.* New York: Academic Press.

Müller, H., Kramm, G., Meixner, F., Dollard, G. J., Fowler, D., Possanzini, M., 1993: Determination of HNO_3 dry deposition by modified Bowen ratio and aerodynamic profile techniques. *Tellus,* **45B**, 346–367.

O'Dell, R. A., Taheri, M., Kabel, R. L., 1977: A model for uptake of pollutants by vegetation. *J. Air Poll. Control Assoc.*, **27**, 1104–1109.

Owen, P. R., Thomson, W. R., 1963: Heat transfer across rough surfaces. *J. Fluid Mech.*, **15**, 321–334.

Paulson, C. A., 1970: The mathematical representation of wind speed and temperature profiles in the unstable atmospheric surface layer. *J. Appl. Meteor.*, **9**, 857–861.

Philip, J. R., De Vries, D. A., 1957: Moisture movement in porous material under temperature gradients. *Trans. Amer. Geophys. Union,* **38**, 222–232.

Phillipps, H., 1962: Zur Theorie des Tagesganges der Temperatur in der bodennahen Atmosphäre und in ihrer Unterlage. *Z. f. Met.*, **16**(5) (in German).

Reichardt, H., 1951: Vollständige Darstellung der turbulenten Geschwindigkeitsverteilung in glatten Rohren. *Z. angew. Math. Mech.*, **31**, 208–219 (in German).

Sasamori, T., 1970: A numerical study of atmospheric and soil boundary layers. *J. Atmos. Sci.*, **27**, 1122–1137.

Schlichting, H., 1965: *Grenzschicht-Theorie.* Karlsruhe. Braun, 5. Aufl., pp. 736 (in German).

Sellers, P. J., 1987: Modeling effects of vegetation on climate. In: Dickinson, R. E., (ed.) *The Geophysiology of Amazonia.* New York, Chichester, Brisbane, Toronto, Singapore: J. Wiley, pp. 297–344.

Sheppard, P. A., 1958: Transfer across the Earth's surface and through the air above. *Quart. J. Roy. Meteor. Soc.*, **84**, 205–224.

Slemr, F., Seiler, W., 1984: Field measurements of NO and NO_2 emissions from fertilized and unfertilized soils. *J. Atmos. Chem.*, **2**, 1–24.

Stockwell, W. R., 1995: Effects of turbulence on gas-phase atmospheric chemistry: Calculation of the relationship between time scales for diffusion and chemical reactions. *Meteorol. Atmos. Phys.*, **57**, 159–171.

Swinbank, W. C., Dyer, A. J., 1967: An experimental study in micro-meteorology. *Quart. J. Roy. Meteor. Soc.*, **93**, 494–500.

Vilà-Guerau de Arellano, J., Duynkerke, P. G., 1993: Second-order closure study of the covariance between chemical reactive species in the surface layer. *J. Atmos. Chem.*, **16**, 145–155.

Ward, D. A., Bunce, J. A., 1986: Novel evidence for a lack of water vapour saturation within the intercellular airspace of turgid leaves of mesophytic species. *J. Experimental Botany,* **37**, 504–516.

Wesely, M. L., Hicks, B. B., 1977: Some factors that affect the deposition rates of sulfur dioxide and similar gases on vegetation. *J. Air Poll. Control Assoc.*, **27**, 1110–1116.

Wesely, M. L., 1989: Parameterization of surface resistances to gaseous dry deposition in regional-scale numerical models. *Atmos. Environ.*, **23**, 1293–1304.

Zdunkowski, W. G., Panhans, W. G., Welch, R. M., Korb, G. J., 1982: A radiation scheme for circulation and climate models. *Beitr. Phys. Atmos.*, **55**, 215–237.

Authors' addresses: G. Kramm, H. Müller, W. Seiler, Fraunhofer-Institut für Atmosphärische Umweltforschung (IFU), Kreuzeckbahnstrasse 19, D-82467 Garmisch-Partenkirchen, Federal Republic of Germany; N. Beier, Meteorologisches Institut der Ludwig-Maximilians-Universität, Theresienstrasse 37, D-80333 München, Federal Republic of Germany; T. Foken, Deutscher Wetterdienst, Meteorologisches Observatorium Lindenberg, Dezernat Landoberflächenprozesse und Grenzschicht, D-15864 Lindenberg, Federal Republic of Germany; P. Schröder, GSF-Research Center, Institute for Plant-Pathology, Building 57, Ingolstädter Landstrasse 1, D-85764 Oberschleißheim, Federal Republic of Germany.